Tellus (1997), 49B, 496–509
Printed in UK – all rights reserved

TELLUS
ISSN 0280–6509

Measurements of arctic sunrise surface ozone depletion events at Kangerlussuaq, Greenland (67°N, 51°W)

By HENRY L. MILLER[1,2]*, ALEX WEAVER[1,2], RYAN W. SANDERS[1], KAREN ARPAG[3] and SUSAN SOLOMON[1], [1]*Aeronomy Laboratory, NOAA,* [2]*CIRES, University of Colorado, Boulder, Colorado, USA,* [3]*Formerly Aeronomy Laboratory and CIRES, USA*

(Manuscript received 17 October 1996; in final form 15 September 1997)

ABSTRACT

In situ measurements of surface ozone were conducted from 30 January through 22 May 1995, at the Sondrestrom Incoherent Scatter Radar Facility near Kangerlussuaq, Greenland. Several periods of depleted ozone were observed, representing the lowest latitude measurements of springtime surface polar ozone depletion in the northern hemisphere to date. The most severe ozone depletion occurred during 14–17 March, when surface ozone levels abruptly fell to below 10 ppbv from typical values of about 40 ppbv. Simultaneous near-ultraviolet and visible total column spectroscopic measurements were made with ground-based instruments, yielding total column values for BrO and OClO. Elevated levels of BrO were observed at the onset of ozone depletion episodes and the behavior of BrO slant column values through the morning twilight of 15 March indicated that the BrO column must reside in the boundary layer. The boundary layer BrO mixing ratio was estimated at greater than 13 pptv during this episode. OClO levels showed no correlation with surface ozone depletion nor clear evidence of a large tropospheric burden.

1. Introduction

During the last decade, interest in levels of atmospheric ozone has been in the forefront of atmospheric science. The discovery of the Antarctic ozone hole, and the effort to understand the underlying causes of this phenomenon captured the attention of much of the scientific community. Of particular interest was that such dramatic and large-scale depletion of stratospheric ozone has been a result of human activity. However, interest in ozone extends to many other geographic and atmospheric regions as well.

One area of interest in particular is the phenomenon of nearly complete removal of boundary layer ozone, or surface ozone, in the Arctic spring. This phenomenon was observed in springtime data from Barrow, Alaska (71.3°N, 156.6°W) (Oltmans, 1981; Oltmans and Komhyr, 1986). Similar observations were found while investigating Arctic haze on northern Ellesmere Island, in Alert, Canada (82.5°N, 62.3°W) (Bottenheim et al., 1986). Low levels of ozone did not correlate with changes in the concentrations of other compounds being studied at that time, and no explanations, either meteorological or chemical, were offered.

Based on a further study in Alert, during April 1986, Barrie et al. (1988) proposed a mechanism to account for polar sunrise surface ozone depletion. A strong anti-correlation was found between surface ozone levels and filterable bromine (f-Br: defined as the sum of particulate and gaseous bromine). This mechanism required isolation of the Arctic boundary layer from the rest of the troposphere and f-Br production within the

* Corresponding author, address: NOAA Aeronomy Lab., 325 Broadway REAL 8, CO80303 Boulder, USA.

boundary layer upon the return of sunlight to the Arctic regions.

A strong temperature inversion commonly found throughout the Arctic during the winter and spring isolates the boundary layer. Bromoform ($CHBr_3$) is the most abundant alkanobromine in the Arctic boundary layer, and the most easily photolyzed (Barrie et al., 1988). Once bromine atoms have been liberated by photolysis, catalytic destruction of ozone can proceed:

$$Br + O_3 \rightarrow BrO + O_2 . \quad (1)$$

The self-reaction of BrO proceeds along one of two pathways to regenerate atomic bromine:

$$BrO + BrO \rightarrow 2Br + O_2 , \quad (2)$$

$$BrO + BrO \rightarrow Br_2 + O_2 , \quad (3a)$$

$$Br_2 \xrightarrow{h\nu} 2Br . \quad (3b)$$

The amount of active bromine is also affected by formation/destruction of reservoirs, such as HOBr. This catalytic cycle continues until the stable inversion layer is destroyed, and free troposphere air mixes with the boundary layer, diluting the concentration of f-Br and replenishing the ozone.

Further studies tend to support this theory. During the Polar Sunrise Experiment 1988, conducted at Alert from February through April 1988, the strong correlation between wind direction, low temperatures, and surface ozone depletion supported the Barrie et al. (1988) inversion hypothesis. Low ozone levels occurred only when winds brought in air from the north and northeast, which had passed over the ice cap (Bottenheim et al., 1990). Again, high levels of f-Br existed during periods of low surface ozone.

In 1992, another Polar Sunrise Experiment was carried out at Alert which included measurements of BrO using long path differential absorption spectroscopy through the troposphere (Hausmann and Platt, 1994). Although there were few BrO measurements, with low temporal resolution due to poor visibility, a weak anti-correlation between BrO levels and surface ozone levels was found. Measured BrO levels varied from 17 pptv down to the detection limit of 4 pptv.

Based upon whole air grab samples collected daily at both Alert and a site on an ice floe 150 km north of Alert, evidence was also found for chlorine atom chemistry during the ozone depletion episodes (Jobson et al., 1994). Chlorine and chlorine-bromine cycles have been found to destroy ozone in the stratosphere (Solomon et al., 1987a; Solomon et al., 1989); similar mechanisms could be involved in surface ozone depletion events. As suggested by Le Bras and Platt (1995), the catalytic ozone destruction cycle involving the reaction of chlorine monoxide with bromine monoxide (McElroy et al., 1986), could compete with the BrO-BrO cycle proposed by Barrie et al. (1988) via reactions 4 through 6 shown below:

$$Cl + O_3 \rightarrow ClO + O_2 , \quad (4)$$

$$ClO + BrO \rightarrow Cl + Br + O_2 , \quad (5)$$

$$ClO + BrO \rightarrow BrCl + O_2 , \quad (6a)$$

$$BrCl \xrightarrow{h\nu} Cl + Br . \quad (6b)$$

An alternate pathway for the reaction of ClO and BrO produces OClO (reaction 7), but does not result in net ozone loss, as the OClO photolysis product, atomic oxygen, will readily combine with O_2 to produce ozone:

$$ClO + BrO \rightarrow OClO + Br , \quad (7)$$

$$OClO \xrightarrow{h\nu} O + ClO . \quad (8)$$

The amount of active chlorine is also regulated by the formation and destruction of reservoirs, particularly HCl.

Sources for both the bromine and chlorine atoms needed to destroy ozone (reactions 1 and 4) are found in the marine environment (Le Bras and Platt, 1995, and references therein). Reactions involving sea salt aerosols and sea ice provide both Br and Cl through a variety of mechanisms (Mozurkewich, 1995; Sander and Crutzen, 1996; Vogt et al., 1996; Tang and McConnell, 1996). Bromoform gas and other short-lived bromocarbons, produced by marine organisms, may also liberate Br via photolysis (Barrie et al., 1988).

Theory, and limited measurements, implicate BrO as a compound of particular interest. In addition, chlorine may play a role in surface ozone depletion events. An existing experiment, near the Arctic circle in Greenland, offered an opportunity to gather more data on conditions surrounding these events. A near-UV/visible spectrograph had already been deployed to the Sondrestrom Incoherent Scatter Radar Facility (SISRF) in

September 1994. Although the site and equipment were chosen and designed for studies of stratospheric chemistry, measurements of differential slant column abundances of BrO, OClO, and NO_2 were conducted, and information pertinent to surface ozone depletion derived.

Deployment of an in situ surface ozone analyzer and a second spectrograph dedicated to column measurements in the near-ultraviolet allowed for examination of atmospheric composition during low tropospheric ozone events, should any occur. This site, located about 10 km west of Kangerlussuaq, Greenland (formerly Sondrestrom AFB), is different from locations at which previous surface ozone depletion events had been measured. It is further south than the other sites, located just north of the Arctic Circle at 67°N. No measurements of surface ozone depletion are previously reported south of 71°N. Indeed, at several sites further south (Edmonton and Goose Bay, Canada, 54°N; Churchill, Canada, 60°N; Westman Islands, Iceland, 63°N; and Finland, 67°N) (Oltmans, 1993; S. J. Oltmans, private communication, 1995) no evidence of this phenomenon was found . At 51°W, Kangerlussuaq is also further inland than other sites, approximately 140 kilometers east of Davis Strait, which lies between Baffin Island and Greenland.

This paper presents the data collected at Kangerlussuaq through the late winter and spring of 1995, as it relates to the phenomenon of polar sunrise surface ozone depletion. The measurements of surface ozone from the end of January through the end of May are shown, as well as the total column BrO data. Column measurements of OClO are discussed, and a brief discussion of the attendant meteorology is presented. Evidence for the presence of tropospheric BrO and limits on the amount of tropospheric OClO are also discussed.

2. Instrumentation

In September 1994, a newly designed and constructed Czerny-Turner spectrograph (herein referred to as SpectA) with a 1024-element Reticon diode-array detector was installed at SISRF. This instrument is equipped with a computer controlled grating, allowing spectroscopic measurements spanning different wavelength intervals. The visible wavelength interval from 402 to 424 nm was chosen for optimal OClO retrieval, with a dispersion of approximately 0.021 nm/diode. SpectA was installed with the optic axis oriented vertically, and the feed optics penetrated the roof. All column OClO measurements discussed here were made using scattered light, in a zenith viewing mode.

In late January 1995, two additional instruments were deployed at SISRF. A crossed Czerny-Turner spectrograph (herein referred to as SpectB), also with a 1024-element Reticon diode-array detector, was placed adjacent to SpectA. This fixed-grating instrument has been used by the Middle Atmosphere Group for the last 10 years, in Antarctica, Greenland, and Colorado. SpectB was configured for measurements in the near-ultraviolet, in a wavelength region spanning 332 to 370 nm, at a dispersion of approximately 0.037 nm/diode; see Sanders et al. (1989) for a further description of this spectrograph. All BrO column measurements presented here were made with SpectB in this configuration.

SpectB was installed with a horizontally oriented optic axis, and the feed optics penetrated the side of the building. A front-surface mirror system allowed the field of view to be directed along the 55°-235° azimuth line. Measurements discussed here were taken in an off-axis viewing mode, with the field of view just above the northeastern horizon at a view zenith angle of 87°. An off-axis view orientation creates a longer view path through the troposphere than a zenith view orientation. At an 87° view zenith angle, the view path through the boundary layer is approximately 20 times greater than the view path for a zenith view orientation. While the presence of clouds can limit the extent of all view paths, as long as the bottom of the clouds are above the altitude of the spectrograph, an off-axis view path through the unobstructed atmosphere below the clouds will be subject to the enhancement described above.

The other instrument was a commercial UV photometric ambient ozone analyzer (Teco model 49 100/103). It was initially installed in the same room as the two spectrographs and sampled outside air brought in from above the peak of the SISRF roof. However, the ozone measurements fluctuated drastically as a result of exhaust from the diesel power generators and vehicles that serviced the site. The generators were located approximately 50 m west of the inlet for the ozone

photometer, while the service road lay about 10 m below the inlet. Local topography forms a bowl-like region, within which the SISRF is located. On 30 January, the ozone photometer was moved to a smaller building located to the south, outside the "bowl" described above. The new location was shielded from the generator exhaust, and was subject to the more general wind flow for the region.

Ambient air was drawn into the ozone instrument through Teflon tubing and fittings, from a filtration fitting mounted approximately 5 m above the ground. The filters removed particulates larger than 6 μm in diameter. Ozone levels were determined by ultraviolet differential absorption, with a measurement made every 2 s. The average of these measurements was recorded once every two minutes. Zero-air calibrations were performed approximately every other day. For zero-air checks, ambient air was drawn in from outside, through a desiccant and granulated activated charcoal (GAC) column to remove ozone, NO_2, SO_2 and hydrocarbons. This processed air was then sampled by the instrument. The ozone level during this check was always within 2 ppbv of zero. A weekly check for inlet line losses was performed by passing zero-air through the ozone generator, and measuring the ozone level at the output of the generator, and the level after the output was shunted up to the inlet and down through the inlet lines. The levels were found to be identical, indicating no ozone losses through reactions on the surfaces of the inlet lines and mechanisms.

3. Observations

Surface ozone data for the 1995 season, from 23 January through 22 May, are shown in Fig. 1. Plotted on this figure are every tenth point from the entire data set, which is comprised of two-minute averages throughout the entire measurement period. The gap during 29–30 January represents the time when the instrument was moved from the initial location to the final location, as discussed above. The gap on 21 April was caused by a malfunction of the recording computer. Data prior to the relocation of the instrument shows a great variability in the local surface ozone levels. As previously mentioned, generator exhaust strongly affected the surface ozone levels at the main facility. Data subsequent to the relocation shows a different behavior of ozone levels.

BrO measurements were made with SpectB in the near-ultraviolet from 21 January to 26 June 1995. Data collected prior to 28 February was taken with the field of view set just above the southwestern horizon, at an 85° zenith angle. Subsequent data was collected with the field of view set just above the northeastern horizon, at an 87° zenith angle.

Total column data are analyzed using a non-linear least squares procedure, as discussed in the analysis section of Sanders (1996). These data are reported as a function of the local solar zenith angle, that is, the solar zenith angle at the latitude, longitude and elevation of the spectrograph. Absorption cross sections used in these analyses were measured in the laboratory with the instruments used in this work. These measured cross sections were scaled to literature values, using the values of Wahner et al. (1988) for BrO and Wahner et al. (1987) for OClO. The near-ultraviolet data for each twilight were analyzed relative to two different references, a daily background and a seasonal background. Analysis against a daily background is useful for providing immediate information about the current composition of the atmosphere, and minimizes difficulties with instrumental drift or inconsistencies, as discussed in Mount et al. (1987) and Solomon et al. (1987a). This style of analysis typically uses either the data record closest to an 80° solar zenith angle as the reference, or the record with the smallest solar zenith angle available for the day.

Later in the season, one data record is chosen as a seasonal background. For the seasonal BrO data presented here, the background was a data record taken at a solar zenith angle of 80.0°, shortly after noon on 14 February. A major advantage to using a seasonal background is that the retrieved differential slant column values for a given species can be directly compared with each other, since the values have been determined relative to the same reference. Usually, a particular spectrum is chosen for use as a seasonal background with the belief that the amount of the compound of interest, in this case BrO, is minimal or below the instrumental detection limit. This determination is made by careful examination of analysis results using a daily background.

In Fig. 2, the analysis results for one near-

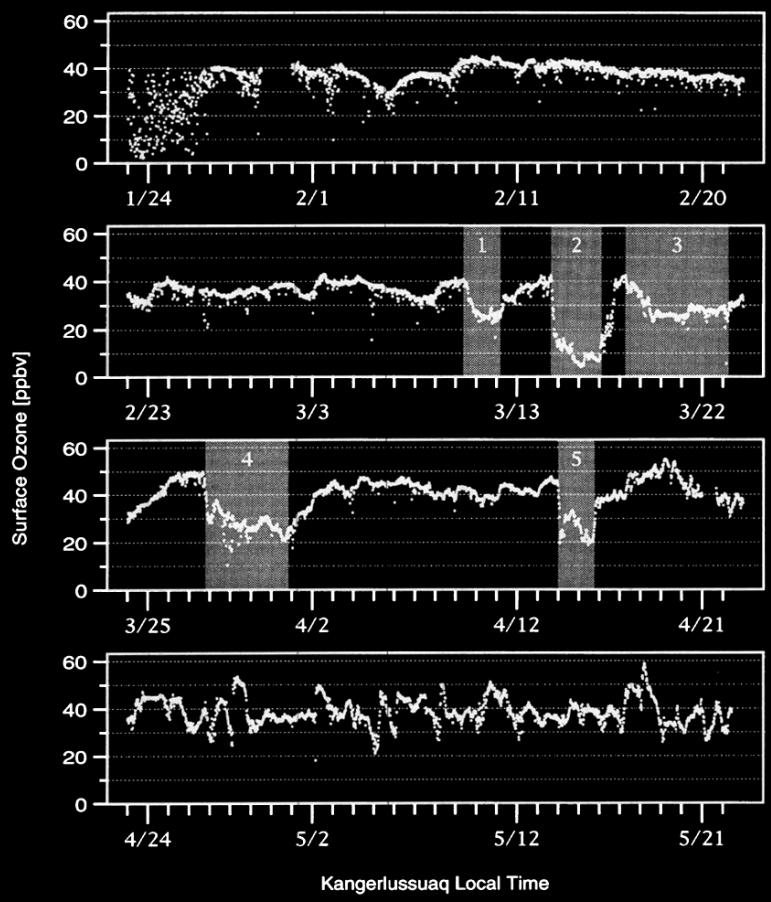

Fig. 1. Surface ozone data during winter and spring of 1995, from Kangerlussuaq, Greenland. Data points recorded every two minutes, as the average of approximately 60 two-second measurements. Every 10th data point recorded is shown here. Data prior to 30 January measured at main site, ensuing data measured at auxiliary site. Major ozone depletion episodes are shaded and labelled 1 through 5.

ultraviolet spectrum relative to the seasonal background used for this work are shown. The residual spectrum, after removal of the absorption effects of NO_2, O_3, OClO, BrO, and O_4, as well as consideration of Rayleigh scattering, Ring effect and instrumental polarization, is shown in the thin solid line trace. The differential absorption spectrum of BrO has been overplotted (large dotted line trace), and shows little correlation with the first residual spectrum. Shown in the thick solid line trace is a residual spectrum in which a similar treatment of the data has been applied, with the exception that BrO absorption has been omitted from the analysis. There is a strong correlation of the second residual spectrum with the BrO absorption spectrum, representing an absorption on the order of 0.6%.

Visible wavelength region measurements appropriate for OClO retrieval were performed every third day. These data were analyzed in a manner similar to the near-ultraviolet data, as discussed above. In Fig. 3, an example of an analysis residual and retrieved OClO change in slant column are shown. The foreground spectrum is one taken at a solar zenith angle of 93.1° during the evening twilight of 6 January 1995, while the reference spectrum was recorded earlier in the same twilight at a solar zenith angle of 89.5°. The thin solid line trace shows the residual when absorption effects due to NO_2, O_3, OClO and O_4 are removed, along

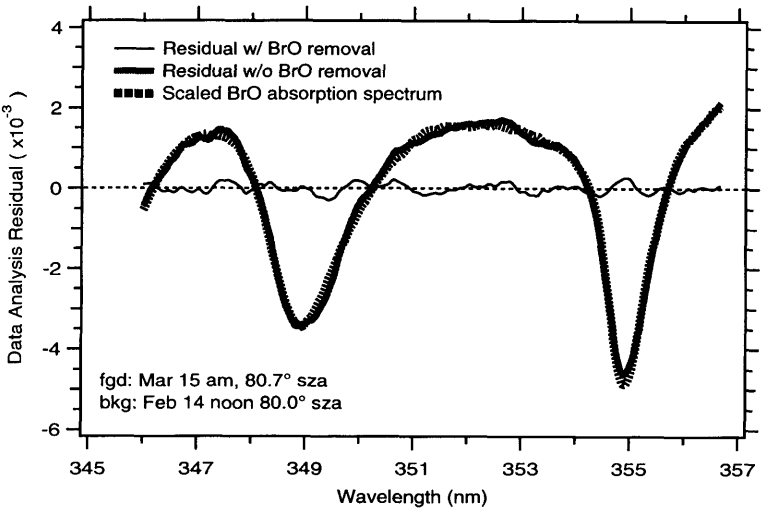

Fig. 2. Analysis for BrO signal in 15 March 80.7° solar zenith angle data record, relative to seasonal background reference spectrum. In the thin solid line residual trace, absorption signatures of NO_2, O_3, BrO, OClO and O_4, as well as the contributions of Rayleigh scattering, Ring effect, and instrumental polarization have been removed. In the thick solid line residual trace, BrO has been omitted from the analysis, and the BrO absorption signature can be clearly seen in the residual spectrum. The BrO absorption spectrum, scaled to the amount found during analysis, is shown in a dotted line trace.

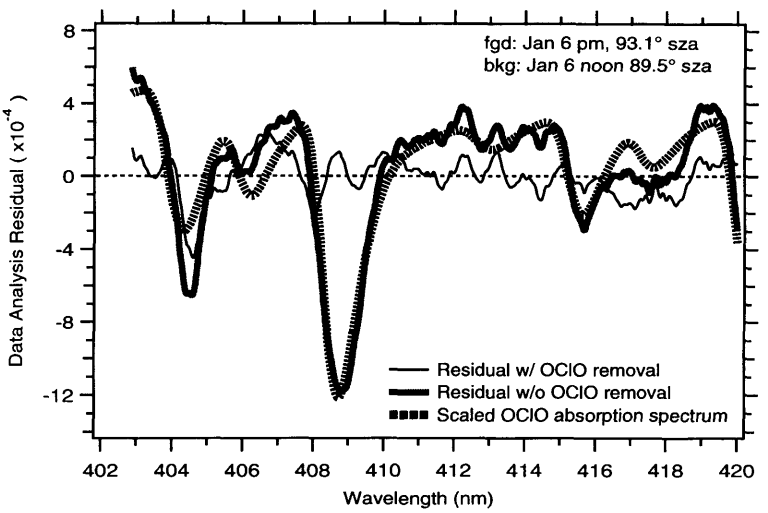

Fig. 3. Analysis residuals of 6 January evening twilight 93.1° solar zenith angle data record, with absorption signatures of NO_2, O_3, and O_4 removed, as well as the contributions of Rayleigh scattering, Ring effect and instrumental polarization. The thin solid line residual trace includes removal of OClO, while the thick solid line residual trace does not. The absorption spectrum of OClO scaled by the amount retrieved is plotted in the dotted line trace.

with the contributions of Rayleigh scattering, instrumental polarization and Ring effect. The OClO absorption spectrum, scaled to the amount indicated in the above retrieval, is plotted in the large dotted line trace. Shown in the thick solid line trace is an analysis residual, in which all the previously mentioned effects except for that of OClO are removed. The absorption of about 0.15%

due to OClO can be quite clearly seen in the residual when OClO is not included in the analysis.

4. Discussion

During the 4 months of surface ozone measurements conducted at Kangerlussuaq, several periods of extended low ozone levels were observed. In Figs. 1 and 4, five major episodes have been labelled (1 through 5). Episode 1 began on the morning of 10 March, with recovery to normal levels beginning in the early morning of 12 March. Episode 2, spanning the period from the afternoon of 14–16 March, was the most severe in extent of ozone depletion, with levels falling to below 10 ppbv. Episode 3, beginning on the morning of 18 March with recovery initiating in the morning of 23 March, spanned the longest time period. Episode 4, from the evening of 27 March into the night of 31 March, also lasted for an extended period of time, while Episode 5, from the very early morning of 14 April through the afternoon of 15 April, was a much more abrupt episode. Episodes 1 and 3 exhibited only marginal ozone depletion, dropping from normal levels to about 30 ppbv, while Episodes 4 and 5 reached lows of about 20 ppbv.

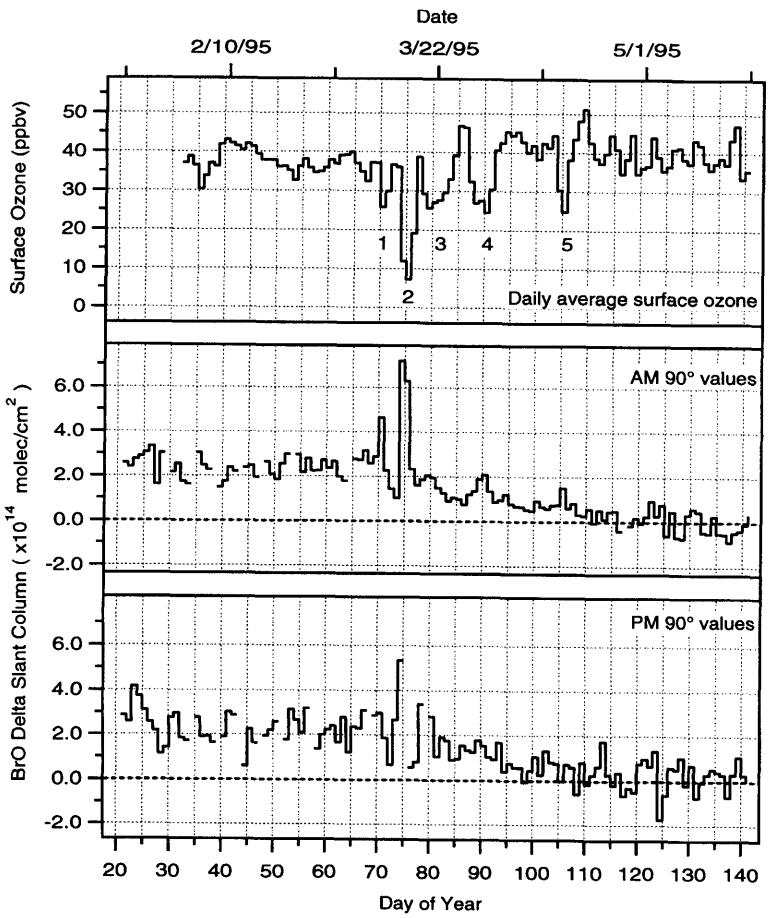

Fig. 4. Daily average of surface ozone levels observed from 1 February–20 May 1995. Off-axis view BrO differential slant column values for the morning and evening twilight 90° solar zenith angles are shown as reduced against a seasonal background. The seasonal reference spectrum is an 80° solar zenith angle data spectrum, collected shortly after noon on 14 February 1995. Episodes 1-5 (see text) are labelled on the surface ozone plot.

In Fig. 4, the daily averages of the surface ozone levels are plotted. Each of the 5 episodes is labelled. Also shown are the morning and evening twilight interpolated 90° solar zenith angle BrO differential slant columns. These data were reduced relative to a seasonal background, taken at 80° solar zenith angle, near noon on 14 February. Gaps in the 90° twilight values occur when the data collected did not span 90°; no extrapolation was performed.

There is a strong anti-correlation of ozone and morning twilight BrO levels during Episodes 1 and 2. The behavior of differential slant column values, hereafter referred to as slant column values, through the morning twilights during Episode 2 indicate that nearly the entire BrO column resides in the boundary layer, as discussed below. At the onset of Episodes 3 through 5, the morning 90° values of BrO are slightly elevated, and the nearly flat response of slant column values with respect to changing solar zenith angle indicate that most of the BrO must be located in the boundary layer.

The most severe ozone depletion occurred in Episode 2, when the daily average fell to about 7 ppbv, with the lowest ozone level during the period falling below 5 ppbv. This episode was accompanied by very high levels of column BrO. The precise concentration of BrO in the boundary layer cannot be determined from these measurements. However, as discussed below, a qualitative argument can be made that the BrO column resides in the lowest part of the atmosphere.

During twilight, slant column values for an absorber located in the stratosphere typically increase with increasing solar zenith angle. Such behavior, due to increasing path length through a stratospheric absorbing layer as the solar zenith angle increases, has been observed many times in the Antarctic (e.g., Solomon et al., 1987b). This response also agrees with predictions based upon models which consider both geometry and photochemistry (Solomon et al., 1989). Such typical stratospheric twilight signatures of OClO were observed in Greenland in early January and during late February and early March. In Fig. 5, an example of this signature is shown for the evening twilight of 21 February.

However, an absorber located low in the troposphere exhibits a very different twilight slant column signature. Single-scattering air mass factor calculations predict that slant column values, relative to an 70° reference, will increase slightly as the solar zenith angle approaches about 80°, and then actually decrease to negative values as the major contribution of the flux reaching the ground shifts to scattering points higher in the atmosphere. For a detailed discussion of intensity-weighted air mass factors and scattering altitudes, see Solomon et al. (1987b) and Perliski and Solomon (1993).

In Fig. 6, two curves illustrating this difference have been drawn. These curves qualitatively depict the fundamental difference in the expected behavior of retrieved slant column values for an absorber located in the boundary layer versus an absorber located in the lower stratosphere. Although these curves represent air mass factor values for the zenith viewing mode, they can be used as a general indicator for the response through twilight of absorbers at these different altitudes. The calculation of off-axis air mass factors has not yet been explicitly performed and is beyond the scope of the present work. However, empirical data exist from Antarctic measurements performed during 1991 (Sanders et al., 1993). In that work, off-axis 80° view angle measurements were intermingled with zenith sky measurements through several twilights. These data were reduced against a seasonal background, obtained in the zenith sky viewing mode. Results show that for an absorber in the middle stratosphere, such as NO_2, there is virtually no change in the observed differential slant column, as most of the absorption due to NO_2 occurred above the scattering altitude. For OClO, which should be predominantly located in the lower stratosphere during the austral spring, there was a slight enhancement due to the use of the off-axis viewing mode, on the order of 30 to 75%. Retrieved values of O_4 showed the greatest change with viewing mode, with a factor of about 3.5 times more O_4 observed in the off-axis viewing mode. The response of O_4 to the change in viewing mode can be used as an indicator of the expected response for an absorbing species located primarily in the boundary layer.

In the bottom panel of Fig. 6, data points for BrO slant column values from the morning twilight of 15 March and the evening twilight of 25 March are also plotted. These data have been reduced against a daily background from earlier in the twilight. The slant column behavior through the 15 March twilight resembles the curve representing an absorber located in the boundary layer.

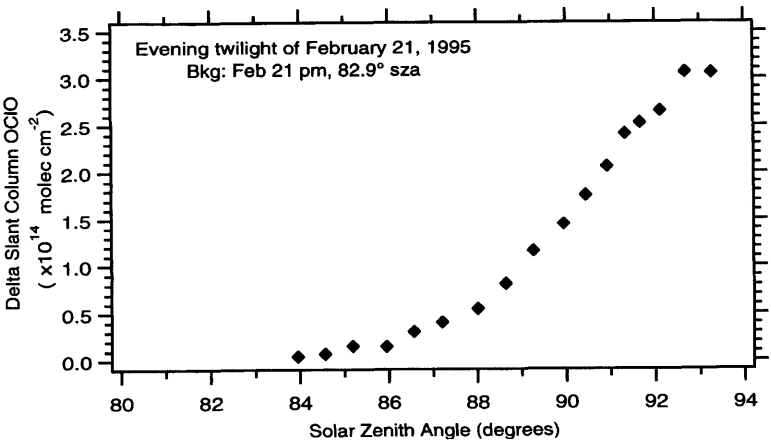

Fig. 5. Retrieved zenith view OClO differential slant columns for the evening twilight of 21 February 1995, using a daily background as reference. Data points exhibit the typical twilight slant column signature for a stratospheric absorber.

The 25 March data, which are representative of more normal levels of surface ozone, show that the bulk of the BrO must reside higher in the atmosphere.

Although the 90° morning BrO values indicate slightly enhanced BrO levels during the onset of all the ozone depletion episodes (Fig. 4), only during the onset of Episode 2 is the behavior of the slant column values clearly indicative of boundary layer BrO. At the beginning of Episode 1, although the total column 90° value is clearly elevated, the behavior of retrieved BrO through the morning twilight indicates that enough BrO resides at higher altitudes to mask the twilight signal of any BrO in the boundary layer. At the beginning of Episodes 3, 4, and 5, BrO levels are not clearly elevated, and the behavior through twilight is much flatter than would be expected for a layer above the lowest kilometer. This may be due to a small amount of BrO located in the stratosphere, with the bulk of the BrO still in the boundary layer. In the air mass factor example used in Fig. 6, at solar zenith angles near 90°, the increased path length through an absorber located in the lower stratosphere is on the order of 20 times greater than the path through an absorber located in the boundary layer. A BrO distribution with 95% in the boundary layer and 5% in the stratosphere could account for a fairly flat response of the retrieved slant column through a twilight, with 90° values only slightly elevated above normal.

When evaluating the amount of a tropospheric species using total column measurements, consideration of path enhancement due to tropospheric clouds must be considered. The potential for an apparent enhancement of a tropospheric absorber exists due to an increase in the tropospheric portion of the light path created by Mie-scattering within the cloud (Erle et al., 1995). If present, such an enhancement would affect all absorbers located in the troposphere, including O_4. Morning twilight data on 13–15 March show that although the BrO levels were clearly elevated throughout the morning of the 15 March, relative to the mornings of 13–14 March, the O_4 signal showed no such change. This strongly supports the view that the enhanced BrO reflects a chemical change.

The BrO measurements are total column data, which do not contain enough information to calculate vertical profiles of BrO. However, an estimate of the BrO concentration can be made, if the vertical extent of the BrO column is assumed. For example, if all the BrO is assumed to be located in the lowest kilometer of the atmosphere, then the concentration can be calculated based on the observation path through that layer. The path length through the lowest kilometer along the instrumental line of sight (view zenith of 87°) is 18.6 km. The retrieved 90° slant column value was

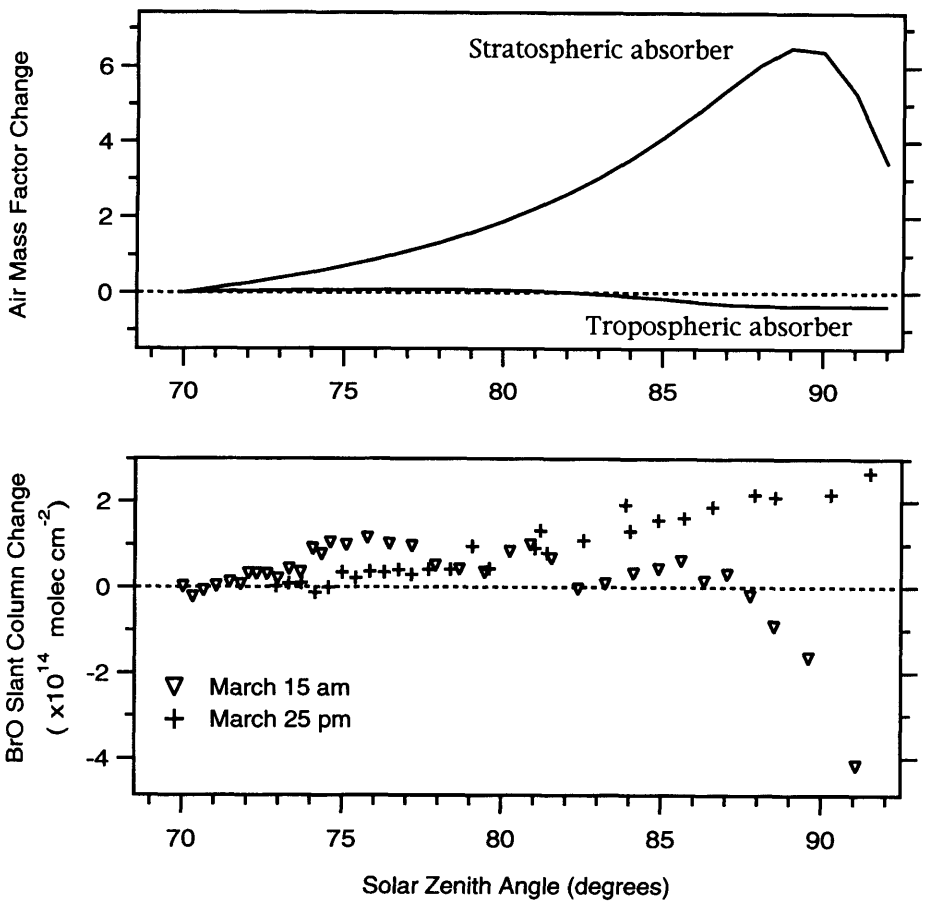

Fig. 6. Characteristic curves of changes in air mass factors from reference for absorbers found in the boundary layer and in the stratosphere are illustrated in the top panel. Plotted below, differential slant column data from 15 March morning twilight indicate that the bulk of the BrO must lie low in the troposphere, while on 25 March the data indicate that the BrO is much higher in the atmosphere.

approximately 6×10^{14} molec cm^{-2}, which converts to a vertical column of about 3.2×10^{13} molec cm^{-2}. This represents a boundary layer concentration of about 3.2×10^{8} molec cm^{-3}, or about 13 pptv. Of course, if the BrO were all in the lowest 500 m, then the concentration in that layer would be double the amount just calculated, or 26 pptv. These estimates agree with the tropospheric long path data published by Hausmann and Platt (1994).

Also consistent with existing theories is the correlation found between surface wind direction and surface ozone depletion. Hourly readings of wind speed and direction by the meteorological staff of the Danish Meteorological Institute (DMI) at the Kangerlussuaq Airport show excellent correspondence between westerly winds and surface ozone depletion events. Fig. 7 shows the wind speed and direction throughout the period of ozone measurements. The periods of low ozone values are labelled to correspond with the labelled episodes shown in Figs. 1, 4. Strong westerly winds bring in air from Davis Strait, where the marine environment can provide the bromine and chlorine necessary for ozone destruction, as previously discussed.

During the late winter and early spring of 1995, the prevailing wind direction is from the northeast,

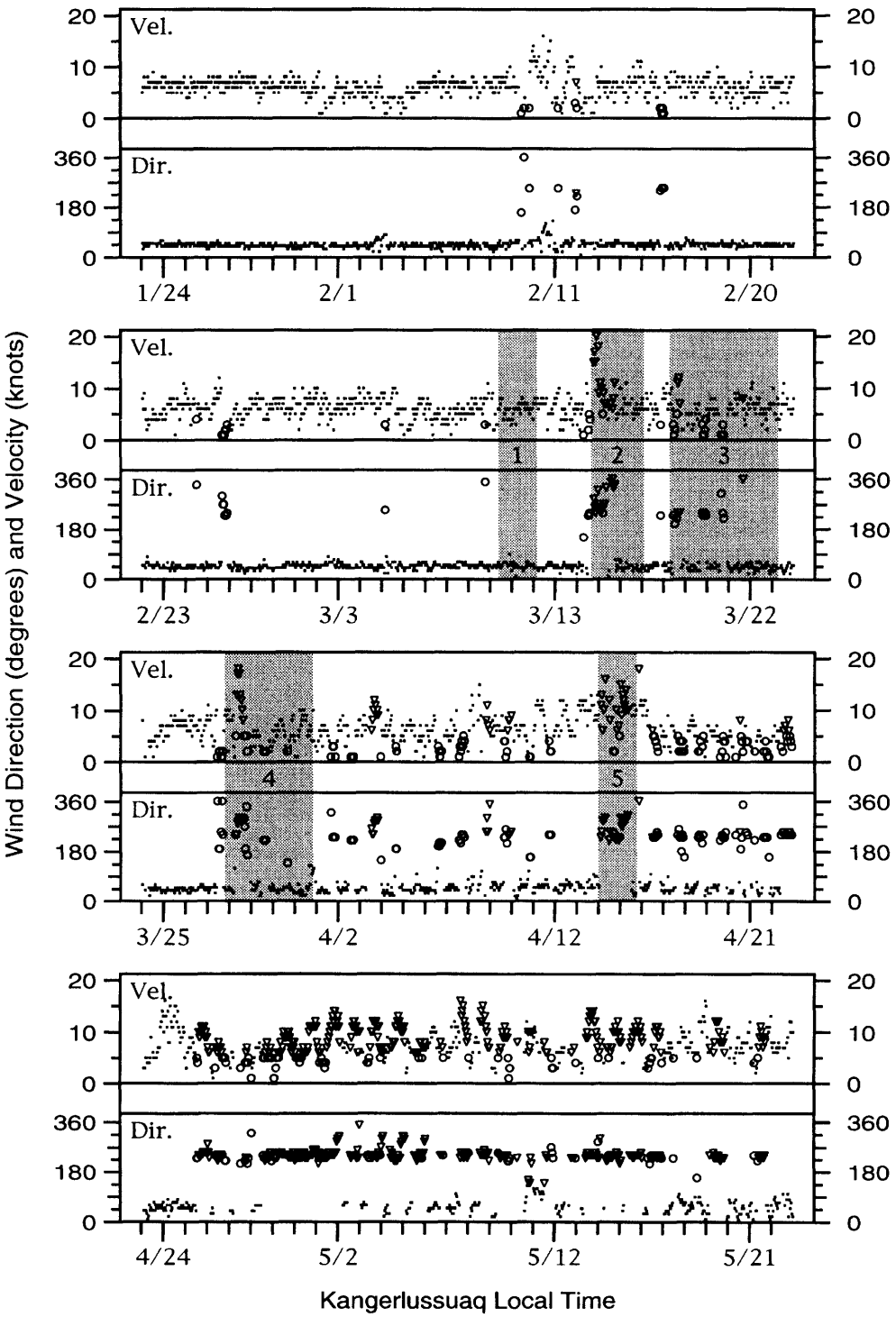

Fig. 7. Wind velocity and direction, as measured at Sondrestrom Airport. Easterly winds are shown as dots, while westerly winds below 5 knots are shown as circles, and westerly winds above 5 knots are shown as triangles. Labelled shaded regions correspond to surface ozone depletion events.

at azimuth angles of about 40° to 60° (Bromwich et al., 1996). These winds move air from the ice cap that covers most of Greenland towards the coast. Throughout late January, February, and March there were only a few periods when the wind shifted from the prevailing direction. In the month of April, these shifts became more frequent, until the winds were predominantly from the southwest.

Concurrent with the onset of each ozone depletion Episodes 2 through 5, winds shifted from the predominant easterlies to higher velocity winds from the southwest, west and northwest. During these initial wind shifts, the velocities are among the highest reported throughout all four months of measurements. At these velocities, air parcels can travel from the coast to Kangerlussuaq in four to five hours. The intervening terrain has many hills, lakes and valleys, with higher peaks near the coast, along the fjord. It is possible that these surface irregularities perturb the boundary layer flow enough to cause some mixing with the ozone-rich free troposphere. Indeed, at no time was total depletion observed in the surface ozone measurements, as observed at the other northern, coastal sites (e.g., Oltmans et al., 1989; Anlauf et al., 1994; Solberg et al., 1996). Except for Episode 2, ozone levels in the air parcels sampled during this study indicate only moderate depletion, if the mechanism of mixing during to transport is not invoked. A more sophisticated meteorological analysis of these episodes has been carried out by Mikkelsen et al. (1996), using back-trajectory calculations to examine air parcel history.

Total column OClO measurements in the visible region (402 to 423 nm) were also conducted throughout the late winter and spring of 1995. During this period, typical stratospheric twilight signatures (Fig. 5) were observed several times, notably during the first three weeks of January, 19–22 February, and 5–9 March. At no time did the retrieved OClO differential slant column show the twilight behavior expected for a boundary layer absorber, as depicted in Fig. 6. Within this wavelength region, the detection limit with this instrument, for a layer of OClO located solely in the lowest kilometer of the troposphere, is on the order of 20 pptv. As discussed for BrO, even a small amount of OClO higher in the atmosphere will mask the presence of tropospheric OClO.

5. Conclusions

During the late winter and spring of 1995, measurements of in situ surface ozone mixing ratio were made in Kangerlussuaq, Greenland, along with ground-based absorption spectroscopy measurements of BrO and OClO differential slant columns. Kangerlussuaq is located at about 67°N, 51°W, just north of the Arctic Circle, near the head of Søndre Strømfjord. The site is approximately 180 m above sea level, approximately 140 km inland from the west coast of Greenland, and about 25 km west of the edge of the Greenland ice cap. In the winter and early spring the surface winds are predominantly easterly, flowing down off the ice cap toward the coast.

During this period, there were several episodes of depleted surface ozone, marked by a rapid decline from normal background levels of about 40 ppbv to 20 ppbv or less. The most dramatic episode began shortly before midnight on 14 March, when surface ozone levels dropped from 40 ppbv to about 10 ppbv within a few hours. Ozone levels remained low throughout 15–16 March, reaching a low of 5 ppbv, with recovery beginning shortly after midnight on 16 March and returning to normal levels by midnight of 17 March. Other episodes of depleted surface ozone spanned the times from 18–23 March, 27 March–1 April, 14–15 April, and, arguably, 10–12 March. On these later occasions, the lowest surface ozone values were on the order of 20 ppbv. At the onset of all but the 10 March episode, the surface winds shifted from predominant easterly direction to higher velocity westerly winds, coming from the coast and Davis Strait.

This data set represents the most southerly measurements of this phenomenon reported to date. Previous surface ozone measurements, from Barrow, Alaska (71°N, 157°W) (Oltmans and Komhyr, 1986; Oltmans et al., 1989; Li et al., 1990), Alert, Canada (82.5°N, 62.3°W) (Bottenheim et al., 1986; Barrie et al., 1988; Mickle et al., 1989; Bottenheim et al., 1990; Anlauf et al., 1994), and Ny-Ålesund, Spitzbergen (78.9°N, 11.9°E) (Solberg et al., 1996), were all taken at high-latitude coastal sites, much closer to the Arctic Ocean and ice cap. The ozone depletion episodes presented in this work are quite apparent, although at no time was the ozone completely depleted as observed in the coastal measurements

mentioned above. This is probably evidence of some mixing of ozone-rich air from the free troposphere during the transport of air parcels inland from the coast (Mikkelsen et al., 1996).

Retrieved differential BrO slant column values show a strong anti-correlation with surface ozone values during the 14–17 March episode. The behavior of the retrieved BrO column throughout the morning twilights during this episode deviates from the characteristic signature of a predominantly stratospheric column. The bulk of the BrO column must reside low in the troposphere in order to explain this deviation from the characteristic twilight signature.

Although the tropospheric BrO concentration cannot be calculated from the total column data presented in this work, the boundary layer concentration can be estimated if an assumption is made about the height of the BrO column. The twilight behavior of BrO indicates that it is low in the troposphere, but the precise thickness of the layer is undetermined. However, if the BrO on the morning of 15 March is assumed to reside uniformly within the lowest kilometer of the atmosphere, the BrO mixing ratio for that layer would have been about 13 pptv. This mixing ratio is comparable to the Alert measurements of Hausmann and Platt (1994).

Retrieved 90° slant column values of BrO indicate slightly elevated levels during the onset of other ozone depletion episodes, but at no other time was the boundary layer twilight signature clear. Indeed, only during times when all, or nearly all, of the BrO column resides in the boundary layer, with therefore minimal contribution to the column from BrO at higher altitudes, does the twilight signature for total column measurements show clear evidence of boundary layer BrO. Most combinations of low altitude BrO with higher altitude BrO mask the low-altitude BrO twighlight signature in total column measurements.

Retrieved values of differential slant column OClO show no correlation with low levels of surface ozone. This is not a conclusive finding with regards to the rôle played in surface ozone depletion by chlorine compounds however, as the instrumental detection limit in this wavelength region for an OClO column of 1 km located at the earth's surface is about 20 pptv. At best, this can be viewed as an upper limit on the boundary layer concentration of OClO. This upper limit does not support a large role for the ClO-BrO reaction in polar sunrise surface ozone depletion.

6. Acknowledgements

The authors wish to thank Dave Parrish and John Holloway of the NOAA Aeronomy Laboratory Tropospheric Chemistry group for the loan of their Teco ozone analyzer and assistance with the Teco operations, as well as Travis Nelson and Matt Warshawsky for processing the surface ozone data. We also thank the DMI staff at the Kangerlussuaq Airport for providing us with daily meteorological data throughout the period of this study. This work could not have been completed without the support of the site crew at the Sondrestrom Incoherent Scatter Radar Facility, operated by SRI International. Finally, we acknowledge the support of DMI, particularly Jens Sohn, Paul Eriksen, Ib Steen Mikkelsen, and Torben Stockflet Jørgensen. This project is funded by the Climate and Global Change Program of the National Oceanic and Atmospheric Administration (NOAA). Logistical and technical support is provided by the National Science Foundation (proposal ID No: DPP-9116717, "UV and Visible Spectroscopy at Three Polar Sites"). We gratefully acknowledge the assistance of the Danish Polar Center's Commission for Scientific Research in Greenland.

REFERENCES

Anlauf, K. G., Mickle, R. E. and Trivett, N. B. 1994. Measurement of ozone during Polar Sunrise Experiment 1992. *Journal of Geophysical Research* **99**, 25 345–25 353.

Barrie, L. A., Bottenheim, J. W., Schnell, R. C., Crutzen, P. J. and Rasmussen, R. A. 1988. Ozone destruction and photochemical reactions at polar sunrise in the lower Arctic atmosphere. *Nature* **334**, 138–141.

Bottenheim, J. W., Gallant, A. G. and Brice, K. A. 1986. Measurements of NO_y species and O_3 at 82° N latitude. *Geophysical Research Letters* **13**, 113–116.

Bottenheim, J. W., Barrie, L. A., Atlas, E., Heidt, L. E., Niki, H., Rasmussen, R. A. and Shepson, P. B. 1990. Depletion of lower tropospheric ozone during Arctic spring: The Polar Sunrise Experiment 1988. *Journal of Geophysical Research* **95**, 18 555–18 568.

Bromwich, D. H., Du, Y. and Hines, K. M. 1996. Wintertime surface winds over the Greenland ice sheet. *Monthly Weather Review* **124**, 1941–1947.

Erle, F., Pfeilsticker, K. and Platt, U. 1995. On the influence of tropospheric clouds on zenith-scattered-light measurements of stratospheric species. *Geophysical Research Letters* **22**, 2725–2728.

Hausmann, M. and Platt, U. 1994. Spectroscopic measurement of bromine oxide and ozone in the high Arctic during Polar Sunrise Experiment 1992. *Journal of Geophysical Research* **99**, 25 399–25 413.

Jobson, B. T., Niki, H., Yokouchi, Y., Bottenheim, J., Hopper, F. and Leaitch, R. 1994. Measurements of C_2-C_6 hydrocarbons during the Polar Sunrise 1992 Experiment: Evidence for Cl atom and Br atom chemistry. *Journal of Geophysical Research* **99**, 25 355–25 368.

Le Bras, G. and Platt, U. 1995. A possible mechanism for combined chlorine and bromine catalyzed destruction of tropospheric ozone in the arctic. *Geophysical Research Letters* **22**, 599–602.

Li, S.-M., Winchester, J. W., Kahl, J. D., Oltmans, S. J., Schnell, R. C. and Sheridan, P. J. 1990. Arctic boundary layer ozone variations associated with nitrate, bromine and meteorology: A case study. *Journal of Geophysical Research* **95**, 22 433–22 440.

McElroy, M. B., Salawitch, R. J., Wofsy, S. C. and Logan, J. A. 1986. Reductions of Antarctic ozone due to synergistic interactions of chlorine and bromine. *Nature* **321** 759–762.

Mickle, R. E., Bottenheim, J. W., Leaitch, W. R. and Evans, W. 1989. Boundary layer ozone depletion during AGASP-II. *Atmospheric Environment* **23**, 2443–2449.

Mikkelsen, I. S., Rasmussen, A., Sorensen, J. H. and Weaver, A. 1996. Surface ozone observations over Greenland. *Conference Proceedings, European Geophysical Society, 21st General Assembly.* The Hague, The Netherlands.

Mount, G. H., Sanders, R. W., Schmeltekopf, A. L. and Solomon, S. 1987. Visible spectroscopy at McMurdo Station, Antarctica, 1, Overview and daily variations of NO_2 and O_3, austral spring, 1986. *Journal of Geophysical Research* **92**, 8 320–8328.

Mozurkewich, M. 1995. Mechanisms for the release of halogens from sea-salt particles by free radical reactions. *Journal of Geophysical Research* **100**, 14 199–14 207.

Oltmans, S. J. 1981. Surface ozone measurements in clean air. *Journal of Geophysical Research* **86**, 1174–1180.

Oltmans, S. J. and Komhyr, W. D. 1986. Surface ozone distributions and variations from 1973–1984 measurements at the NOAA Geophysical Monitoring for Climatic Change Baseline Observatories. *Journal of Geophysical Research* **91**, 5229–5236.

Oltmans, S. J., Schnell, R. C., Sheridan, P. J., Peterson, R. E., Li, S.-M., Winchester, J. W., Tans, P. P., Sturges, W. T., Kahl, J. D. and Barrie, L. A. 1989. Seasonal surface ozone and filterable bromine relationship in the high Arctic. *Atmospheric Environment* **23**, 2431–2441.

Oltmans, S. J. 1993. Climatology of Arctic and Antarctic tropospheric ozone. In: *The tropospheric chemistry of ozone in the polar regions* (eds. H. Niki, H. Becker). Springer-Verlag, Berlin, 25–40.

Perliski, L. M. and Solomon, S. 1993. On the evaluation of air mass factors for atmospheric near-ultraviolet and visible absorption spectroscopy. *Journal of Geophysical Research* **98**, 10 363–10 374.

Sander, R. and Crutzen, P. J. 1996. Model study indicating halogen activation and ozone destruction in polluted air masses transported to the sea. *Journal of Geophysical Research* **101**, 9121–9138.

Sanders, R. W., Solomon, S., Carroll, M. A. and Schmeltekopf, A. L. 1989. Visible and near-ultraviolet spectroscopy at McMurdo Station, Antarctica, 4, Overview and daily measurements of NO_2, O_3, and OClO during 1987. *Journal of Geophysical Research* **94**, 11 381–11 391.

Sanders, R. W., Solomon, S., Smith, J. P., Perliski, L., Miller, H. L., Mount, G. H., Keys, J. G. and Schmeltekopf, A. L. 1993. Visible and near-ultraviolet spectroscopy at McMurdo Station, Antarctica, 9, Observations of OClO from April to October 1991. *Journal of Geophysical Research* **98**, 7219–7228.

Sanders, R. W. 1996. Improved analysis of atmospheric absorption spectra by including the temperature dependence of NO_2. *Journal of Geophysical Research* **101**, 20 945–20 952.

Solberg, S., Schmidbauer, N., Semb, A. and Stordal, F. 1996. Boundary-layer ozone depletion as seen in the Norwegian Arctic in spring. *Journal of Atmospheric Chemistry* **23**, 301–322.

Solomon, S., Mount, G. H., Sanders, R. W. and Schmeltekopf, A. L. 1987a. Visible spectroscopy at McMurdo Station, Antarctica, 2, Observations of OClO. *Journal of Geophysical Research* **92**, 8 329–8 338.

Solomon, S., Schmeltekopf, A. L. and Sanders, R. W. 1987b. On the interpretation of zenith sky absorption measurements. *Journal of Geophysical Research* **92**, 8 311–8 319.

Solomon, S., Sanders, R. W., Carroll, M. A. and Schmeltekopf, A. L. 1989. Visible and near-ultraviolet spectroscopy at McMurdo Station, Antarctica, 5, Diurnal variations of OClO and BrO. *Journal of Geophysical Research* **94**, 11 393–11 403.

Tang, T. and McConnell, J. C. 1996. Autocatalytic release of bromine from Arctic snow pack during polar sunrise. *Geophysical Research Letters* **23**, 2633–2636.

Vogt, R., Crutzen, P. J. and Sander, R. 1996. A mechanism for halogen release from sea-salt aerosol in the remote marine boundary layer. *Nature* **383**, 327–330.

Wahner, A., Tyndall, G. S. and Ravishankara, A. R. 1987. Absorption cross sections for OClO as a function of temperature in the wavelength range from 240–480 nm. *Journal Physical Chemistry* **91**, 2734–2738.

Wahner, A., Ravishankara, A. R., Sander, S. P. and Friedl, R. R. 1988. Absorption cross section of BrO between 312 and 385 nm at 298 and 223 K. *Chemical Physics Letters* **152**, 507–512.